Available online at www.sciencedirect.com
ScienceDirect
Virology 370 (2008) 373–381
VIROLOGY
www.elsevier.com/locate/yviro

Role of phosphorylation clusters in the biology of the coronavirus infectious bronchitis virus nucleocapsid protein

Kelly-Anne Spencer [a], Michael Dee [b], Paul Britton [b], Julian A. Hiscox [a,c,*]

[a] Institute of Molecular and Cellular Biology, Faculty of Biological Sciences, University of Leeds, Leeds, LS2 9JT, UK
[b] Division of Microbiology, Institute for Animal Health, Compton, Newbury, Berkshire, RG20 7NN, UK
[c] Astbury Centre for Structural Molecular Biology, University of Leeds, Leeds, LS2 9JT, UK

Received 16 July 2007; returned to author for revision 11 August 2007; accepted 16 August 2007
Available online 1 November 2007

Abstract

The coronavirus infectious bronchitis virus (IBV) nucleocapsid (N) protein is an RNA binding protein which is phosphorylated at two conserved clusters. Kinetic analysis of RNA binding indicated that the C-terminal phosphorylation cluster was involved in the recognition of viral RNA from non-viral RNA. The IBV N protein has been found to be essential for the successful recovery of IBV using reverse genetics systems. Rescue experiments indicated that phosphorylated N protein recovered infectious IBV more efficiently when compared to modified N proteins either partially or non-phosphorylated. Our data indicate that the phosphorylated form of the IBV N protein plays a role in virus biology.

Keywords: Coronavirus; RNA binding; Nucleocapsid protein; IBV; Surface plasmon resonance; Phosphorylation

Introduction

One of the fundamental stages in the life cycle of coronaviruses and other RNA viruses is the recognition of viral genomic RNA by the virus encoded nucleocapsid protein, for roles in RNA synthesis, encapsidation, packaging and in the correct folding of the RNA molecule. Phosphorylation of the nucleocapsid protein is thought to regulate many of these events although precise roles remain unclear. Coronaviruses are a group of positive strand RNA viruses which cause principally respiratory and gastro-intestinal infections and include the severe acute respiratory syndrome coronavirus (SARS-CoV) (Peiris et al., 2004) and avian infectious bronchitis virus (IBV) (Cavanagh, 2005).

Coronavirus genomes are approximately 30 kb in length, making them the largest RNA genomes so far discovered. Both RNA replication and mRNA transcription occur in virus infected cells and a series of subgenomic mRNA molecules are synthesized by the viral replicase via a discontinuous transcription mechanism (Enjuanes et al., 2006a; Pasternak et al., 2006; Sawicki et al., 2007), in which a viral leader sequence, derived from the 5′ end of the genome, is added to the 5′ end of each subgenomic mRNA (Masters, 2006). Adjacent to the leader sequence is a transcription regulatory sequence (TRS) which also precedes each open reading frame along the genome. Genetic analysis suggests that the TRS and flanking sequences are involved in the modulation of transcription (Alonso et al., 2002; Hiscox et al., 1995; Sola et al., 2005; Van Marle et al., 1995; Zuniga et al., 2004). The TRS has been shown to act as a high affinity binding site for the coronavirus nucleocapsid (N) protein suggesting a role for N protein in transcription (Baric et al., 1988; Nelson et al., 2000; Spencer and Hiscox, 2006a; Stohlman et al., 1988). Although replication can take place without N protein it does so at reduced efficiency (Almazan et al., 2004; Schelle et al., 2005). Furthermore N protein has been shown to co-localize with coronavirus replication complexes in the cytoplasm at early points post-infection (Denison et al., 1999; Van der Meer et al., 1999). Moreover, N protein is required for the efficient rescue of coronavirus genomic RNA from cDNA clones (Almazan et al., 2004; Coley et al., 2005;

* Corresponding author. Institute of Molecular and Cellular Biology, Faculty of Biological Sciences, University of Leeds, Leeds, LS2 9JT, UK.
E-mail address: j.a.hiscox@leeds.ac.uk (J.A. Hiscox).

0042-6822/$ - see front matter © 2007 Elsevier Inc. All rights reserved.
doi:10.1016/j.virol.2007.08.016

Schelle et al., 2005; Yount et al., 2000, 2003) and has been shown to be essential for the rescue of IBV using at least two different types of reverse genetics systems (Britton et al., 2005; Casais et al., 2001; Youn et al., 2005a,b).

Coronavirus N proteins have roles in both virus RNA synthesis and modulating host cell processes and phosphorylation may regulate these processes by exposing various functional motifs (You et al., 2005, 2007). By amino acid sequence comparison coronavirus N proteins can be separated into three regions of conserved homology (Parker and Masters, 1990). Situated within these regions are motifs which play a role in both aspects of virus biology. For example, IBV N protein contains an RNA binding site (Tan et al., 2006), a nucleolar localization signal (Reed et al., 2006) and a nuclear export signal (Reed et al., 2007). These latter two signals modulate its dynamic trafficking (Cawood et al., 2007) between the cytoplasm (the site of viral RNA synthesis) and the nucleolus, suggesting a nucleolar aspect to the virus life cycle (Hiscox, 2007).

Recent studies have shown that the N-terminal region RNA binding site of IBV N protein has the potential to form an electrostatic interaction with RNA (Fan et al., 2005). This was subsequently confirmed by measuring dynamic interactions (using surface plasmon resonance (SPR)) (Spencer and Hiscox, 2006a) and raised the possibility that N protein initially bound viral RNA via a weak electrostatic interaction (a 'lure' step) and that a 'lock' step was facilitated by specific high affinity binding to structures on the viral RNA such as the TRS (Spencer and Hiscox, 2006a). This latter stage being similar to the recognition of the hantavirus vRNA panhandle by its nucleocapsid protein (Mir et al., 2006) or the interaction of HIV-1 Rev protein with loop A (Greatorex et al., 2006). Again, similar to the ability of the hantavirus nucleocapsid protein (Mir and Panganiban, 2006), the coronavirus N protein has also been shown to have RNA chaperone activity (Zuniga et al., 2007).

IBV N protein has a predicted molecular weight of 45 kDa, although migrates under SDS–PAGE with a mobility of ~50 kDa, suggestive of post-translational modifications (Chen et al., 2003), which was confirmed by the incorporation of ^{32}P-orthophosphate into N protein during infection and was also found in virions (Jayaram et al., 2005). Although coronavirus N proteins were predicted to be phosphorylated at multiple serine residues, mass spectroscopic analyses identified two regions of phosphorylation on the IBV N protein (when over-expressed) which are located at two conserved amino acid clusters, Ser^{190} and Ser^{192} and Thr^{378} and Ser^{379} (Chen et al., 2005). The protein was heterogeneously phosphorylated with the predominant species having all four sites occupied (Chen et al., 2005), which reflects the mobility of IBV N protein (detected using western blot) during infection, in which a single N protein species is observed (Dove et al., 2006). Similarly the porcine coronavirus, transmissible gastroenteritis virus (TGEV), N protein was also found to be phosphorylated at two clusters, amino acids Ser^{156}, Ser^{254} and Ser^{256} (Calvo et al., 2005). The murine coronavirus, mouse hepatitis virus N protein is phosphorylated at Ser^{170}, Thr^{177}, Ser^{389}, Ser^{424} and Thr^{428} (White et al., 2007). Although the precise sites have not been mapped, the SARS-CoV N protein is thought to be phosphorylated at serine residues (Surjit et al., 2005). Thus for IBV and MHV N proteins these phosphate groups are located in the middle and C-terminal regions of the protein, and overall the IBV, TGEV and MHV analyses demonstrate that coronavirus N proteins are phosphorylated but not at multiple (<10) serine residues which was once accepted dogma based upon prediction analysis.

Kinetic analysis indicated that phosphorylation of the IBV N protein played a role in discriminating between non-viral (random RNA) and IBV RNA (the leader sequence); the phosphorylated N protein having a high binding affinity for viral RNA compared to non-viral RNA (Chen et al., 2005). In contrast, non-phosphorylated N protein bound to either viral or non-viral RNA with similar affinities (Chen et al., 2005).

However, given the conserved nature of N protein phosphorylation, the role of whether both or single phosphorylation clusters mediated RNA binding and the general role of phosphorylation of N protein in virus biology has not previously been elucidated and is addressed in this study.

Results and discussion

Generation and characterization of differentially phosphorylated N proteins

To investigate the role of the phosphorylation clusters in the binding of IBV N protein to RNA and in the biology of virus replication, site directed mutagenesis was used to replace the appropriate amino acid coding sequences in the IBV N gene sequence in the expression plasmid pTriExIBVN, generating plasmids pTriExIBVN$_{SSAA}$, pTriExIBVN$_{AATS}$ and pTriExIBVN$_{AAAA}$; all with a C-terminal his-tag coding sequence for protein purification purposes. Plasmid pTriExIBVN had previously been used to make a recombinant baculovirus for expressing phosphorylated IBV N protein in Sf9 cells (referred here as N$_{SSTS}$) (Chen et al., 2003, 2002). Previous mass spectroscopic analysis demonstrated that N protein expressed in insect cells had identical post-translational modifications to that produced in a cell line (Vero) permissive to virus infection (Chen et al., 2005). A similar approach was used in this study to generate recombinant baculoviruses for the expression of modified IBV N proteins. The baculoviruses were used to express modified N proteins in which either Ser^{190} and Ser^{192} (N$_{AATS}$) or Thr^{378} and Ser^{379} (N$_{SSAA}$) were substituted for the amino acid alanine resulting in a partially phosphorylated IBV N protein. A third recombinant baculovirus was produced that expressed a modified N protein in which all four amino acids were substituted for alanine resulting in a non-phosphorylated (N$_{AAAA}$) form of the IBV N protein. The N$_{AAAA}$ protein was used in place of *E. coli* expressed N protein (non-phosphorylated protein) to ensure that any additional post-translational modifications, such as acetylation, were present.

The modified IBV N proteins were purified by nickel affinity chromatography and analysis of the recombinant purified proteins using SDS–PAGE indicated that N$_{SSAA}$ and N$_{AATS}$ had identical mobility, whereas N$_{AAAA}$ had the fastest mobility

and was equivalent to protein expressed in *E. coli* (and therefore non-phosphorylated) and N_{SSTS} had the slowest mobility (Fig. 1). These differences in electrophoretic mobility suggested that the purified proteins were phosphorylated to different extents and these differences are distinguishable due to the additional charge that is added to the protein upon phosphorylation. As predicted N_{SSAA} and N_{AATS} had identical mobility as both contained two phosphate groups.

To confirm this, native phosphorylated N protein and the three phosphorylation mutants were subject to in-gel tryptic digestion and the resulting peptide pools separated using a C18 column and eluent analyzed by electrospray MS/MS. The analysis confirmed that as in the previous study (Chen et al., 2005) all four sites on N_{SSTS} could be phosphorylated (data not shown) and confirmed that on N_{AAAA} Ser^{190} and Ser^{192} and Thr^{378} and Ser^{379} were all replaced with alanine and no other phosphorylation occurred (data not shown). N_{SSAA} and N_{AATS} were bi-phosphorylated as the predominant species (data not shown) which was also reflected in their identical electrophoretic mobility (Fig. 1).

Role of phosphorylation clusters in the recognition of IBV RNA by IBV N protein

SPR analysis was used to investigate the relative role or contribution of either the region II phosphorylation cluster or region III phosphorylation cluster in the recognition of RNA by N protein as described previously (Chen et al., 2005; Spencer and Hiscox, 2006a). Briefly, the biotinylated RNA sequences were immobilized separately on a streptavidin sensor chip (BIAcore) and 3.125, 6.25, 12.5, 25, 50 and 100 nM concentrations of the modified IBV N proteins were allowed to interact with the target RNAs in a liquid phase. Each protein concentration was injected in duplicate and the experiment repeated three times. The resultant sensograms were analyzed using BIAevaluation software (BIAcore) as described previously (Chen et al., 2005; Spencer and Hiscox, 2006a).

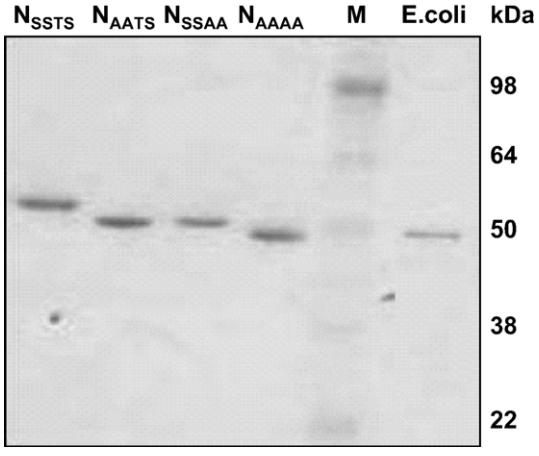

Fig. 1. Comparison of the mobility using SDS–PAGE between phosphorylated IBV N protein (N_{SSTS}), N_{AATS} protein, N_{SSAA} protein, N_{AAAA} protein and N protein expressed in *E. coli* (Spencer and Hiscox, 2006a). Molecular weights are indicated to the right and the appropriate ladder is denoted (M).

The data fitted to a 1:1 Langmuir binding model and indicated that all four IBV N proteins, N_{SSTS}, N_{SSAA}, N_{SSAA} and N_{AAAA}, had high affinity binding, K_D=1.7–3.5 nM, to the viral-derived RNA, with no significant difference between the overall binding affinities (Fig. 2, Table 1). The baculovirus-derived phosphorylated viral N protein (N_{SSTS}) bound to the viral RNA with high affinity (K_D=2.8 nM), but in contrast bound with approximately 900 times lower affinity (K_D=2510 nM) to the random RNA (Fig. 3, Table 1). This difference in affinity resulted from decreased association and increased dissociation rates for random versus viral RNA. The non-phosphorylated IBV N protein, N_{AAAA}, and the partially phosphorylated N protein, N_{SSAA}, bound non-viral RNA with higher affinities. However, the partially phosphorylated N protein, N_{AATS}, bound non-viral RNA with approximately 246 times lower affinity than the non-phosphorylated N_{AAAA} protein, with binding kinetics similar to the phosphorylated N_{SSTS} protein (Fig. 3, Table 1). These data indicated that phosphorylation of the amino acids Thr^{378} and Ser^{379} of the IBV N protein was involved in discrimination of viral from non-viral RNA.

In many cases phosphorylation of a capsid protein has been shown to be involved in regulating RNA binding and in general two different mechanisms may be in operation. In the first case phosphorylation through altering charge may affect binding affinity. For example, dephosphorylation of the rubella virus capsid protein increases its binding affinity for viral RNA and specific phosphorylation sites are involved in the process (Law et al., 2003). This is also the case for IBV N protein where non-phosphorylated N protein can bind viral RNA with higher affinity than phosphorylated protein, but at the expense of specificity. Likewise, phosphorylation has been proposed to reduce the electrostatic interaction with target RNA, as in the case of the binding of potato virus A coat protein to RNA (Ivanov et al., 2001). Given the binding differences between N_{AATS} protein and N_{SSAA} protein for viral RNA it can be concluded that overall negative charge is not contributing to binding, otherwise the two proteins would have equivalent binding kinetics. Both of these proteins had identical motilities as determined by SDS–PAGE analysis (Fig. 1), and again mass spectroscopy confirmed their phosphorylation status with two phosphorylated sites.

Phosphorylation of N protein does not affect the overall structure

An alternative mechanism is that phosphorylation can affect the conformation of a protein with a corresponding effect on RNA binding properties, as in the case of human immunodeficiency virus type 1 Rev protein, where the phosphorylation of one or two serine residues can cause the closure of an RNA binding cleft in the protein (Fouts et al., 1997). Similarly, phosphorylation of the duck hepatitis B virus capsid protein causes a conformational change in the C-terminal region of the protein (Yu and Summers, 1994). In order to determine whether there were any major conformational differences in the N protein structures between the modified forms of the N proteins

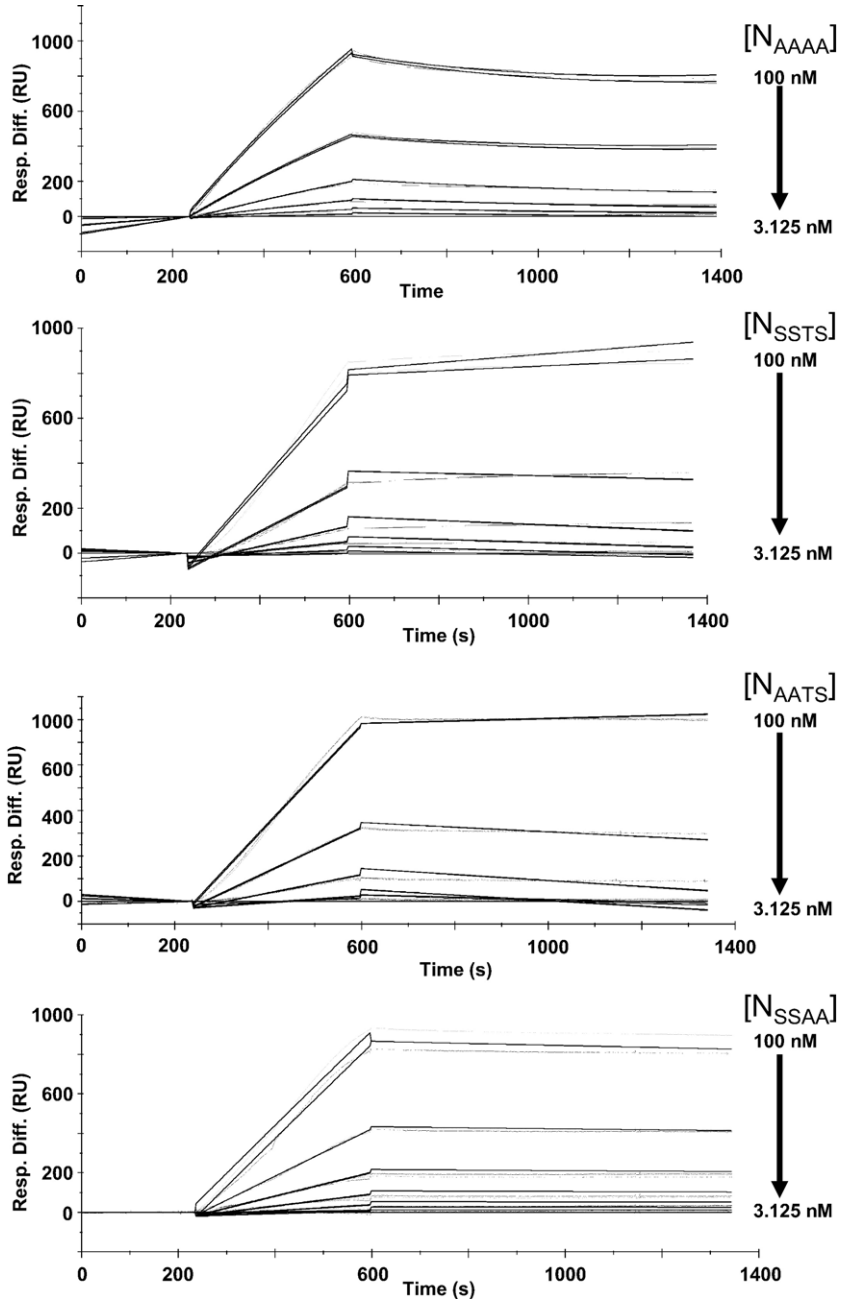

Fig. 2. Kinetic analyses of IBV N protein and the N proteins with modified sites binding to viral RNA. The proteins at 3.125, 6.25, 12.5, 25, 50 and 100 nM concentrations were injected over the immobilized RNA; association was monitored for 6 min followed by a 12 min dissociation phase. Black lines represent fitted data. Kinetic parameters for the experiments are shown in Table 1.

either following loss of the phosphate group from substitution of the Ser or Thr amino acids with Ala, circular dichroism (CD) spectroscopy was used to determine the conformational states of the four N proteins. CD spectroscopy results in the detection of changes in the overall secondary structure of a protein. CD spectroscopic measurements were taken in the far UV (180–260 nm) spectra. This was repeated three times for all four proteins with different protein samples used in each separate experiment. The HT reading was taken along side all measurements to ensure that the signal to noise ratio remained below the level at which data could be considered reliable. An example of a CD spectrum obtained for all four proteins with the average HT reading for all four proteins is shown in Fig. 4. The resulting data (above a wavelength of 195 nm) indicated that the differing phosphorylation patterns did not result in different overall secondary structures, as judged by the similarity of the four CD readings produced. The spectra of all four proteins remained below the axis for the majority of the reading, with a major trough occurring between 200 and 210 nm. One subtle difference that can be observed is that the CD trace of both the partially phosphorylated proteins remained slightly closer to the *x*-axis (i.e. less negative) between 250 and 200 nm than the same region of the fully and non-phosphorylated proteins. Despite this difference in magnitude of the CD signals, the general shapes of

Table 1
Average kinetic parameters for IBV N protein and phosphorylation mutants interacting with viral and non-viral RNA

	k_{ass}	k_{diss}	K_D (nM) [a]	χ^2
Viral RNA				
N_{SSTS}	$5.5\pm1.0\times10^{3}$	$1.6\pm0.9\times10^{-5}$	2.8±1.3	6.13
N_{AATS}	$5.5\pm1.3\times10^{3}$	$1.2\pm0.6\times10^{-5}$	2.2±0.7	2.97
N_{SSAA}	$5.2\pm0.7\times10^{3}$	$8.6\pm1.3\times10^{-6}$	1.7±0.7	0.639
N_{AAAA}	$2.1\pm0.4\times10^{4}$	$7.3\pm0.9\times10^{-6}$	3.50±0.84	0.379
Non-viral RNA				
N_{SSTS}	$9.4\pm0.6\times10^{2}$	$2.3\pm0.1\times10^{-3}$	2510±18.4	4.9
N_{AATS}	$3.1\pm1.3\times10^{2}$	$1.4\pm0.1\times10^{-3}$	4670±20.7	8.06
N_{SSAA}	$2.1\pm0.7\times10^{3}$	$2.3\pm1.3\times10^{-4}$	111±7.36	10.3
N_{AAAA}	$6.8\pm0.8\times10^{3}$	$1.3\pm0.3\times10^{-4}$	19.1±4.11	11.5

[a] K_D values were calculated from the k_{diss} and k_{ass} ratios ($K_D=k_{diss}/k_{ass}$) and the errors of K_D (EK_D) were calculated from the errors of k_{ass} (Ek_{ass}) and k_{diss} (Ek_{diss}) using the equation

$$EK_D = K_D\sqrt{\left(\frac{Ek_{diss}}{k_{diss}}\right)^2+\left(\frac{Ek_{ass}}{k_{ass}}\right)^2}.$$

the spectrum remain similar. Moreover, the trend of remaining negative and evoking a major trough peaking at approximately 208 nm was the same as observed in the far CD spectrum of IBV N protein expressed and purified from *E. coli* (Spencer and Hiscox, 2006a).

In order to statistically test the observation that phosphorylation status did not alter the gross conformation of IBV N protein, CD data were analyzed by a number of algorithms provided by the DICHROWEB on-line server (Whitmore and Wallace, 2004). As for previous analysis (Spencer and Hiscox, 2006a) the CDDSTR (a Fortran program (Johnson, 1999)) provided the best fitting data, as judged by the low normalized root mean square deviation (NRMSD) values and close agreement between the experimental and reconstructed spectra. As such, data estimated by this method were used to compare the structures of differentially phosphorylated N proteins (Table 2). The data indicated that all four proteins were made up of a large proportion of β structures, with β-sheets and turns accounting for over 50% of the secondary structure. The proteins contained an average of 20% α-helix with the remaining 26–27% being comprised of random coil structures, again these are consistent with those estimations of secondary structure for (non-phosphorylated) N protein expressed in *E. coli* (Spencer and Hiscox, 2006a). The Student's *t*-test revealed that any difference between the secondary structure elements of the differentially phosphorylated B proteins was not significant (data not shown). These proportions are in approximate agreement with the solid state structure for the N and C-terminal regions of IBV N protein (Jayaram et al., 2006).

Ability of differentially phosphorylated N protein to rescue infectious IBV from cDNA

To investigate whether the phosphorylation status of N protein played a role in the biology of IBV this study utilized modified IBV N proteins to rescue infectious IBV using the reverse genetics system for IBV (Fig. 5), as described (Casais et al., 2003, 2001). N protein is essential for the successful rescue of IBV using at least two different types of reverse genetics systems (Britton et al., 2005; Casais et al., 2001; Youn et al., 2005a,b). Recovery of infectious IBV was repeatedly found to be unsuccessful in the absence of the IBV N protein or from the use of an IBV N gene that lacked the correct initiation codon for the N protein. However, infectious IBV was rescued via co-transfection of plasmid DNA expressing either IBV N_{SSTS}, N_{SSAA}, N_{AATS} or N_{AAAA} (pCi-NeoIBVN_{SSTS}, pCi-NeoIBVN_{SSAA}, pCi-NeoIBVN_{AATS} and pCi-NeoIBVN_{AAAA}, respectively) and vaccinia virus DNA containing a full-length IBV cDNA under the control of a T7 promoter sequence in chick kidney cells previously infected with a recombinant fowlpox virus expressing T7 RNA polymerase. The rescue experiments were repeated three times. The amounts of progeny virus rescued in the transfected cells were determined by plaque assay, as an approximate determination of the efficiency of rescue, and related to input plasmid, generating a numerical output of infectious units per μg of input plasmid. All of the modified N proteins resulted in the rescue of infectious IBV, indicating that phosphorylation of the IBV N protein is not required for this biological activity. However, analysis of the rescue of infectious IBV indicated that the IBV N proteins N_{SSTS}, N_{SSAA}, N_{AATS} and N_{AAAA}, generated 3200±154, 25±6, 680±17 and 68±9 infectious units per μg of input plasmid, respectively.

As controls, plasmids in which the initiation codon, AUG, of N protein had been mutated and therefore did not express the IBV N protein or plasmids expressing the influenza virus nucleoprotein (pcDNA2.1-NP-wt) or the bovine viral diarrhea virus capsid protein (pEF6A-BVDV-capsid) were incapable of rescuing infectious IBV (data not shown). This indicated that although the phosphorylated form of the IBV N protein was not required for rescue of IBV it was, however, more efficient for rescue, when compared to partially phosphorylated or non-phosphorylated forms of the N protein, indicating some role for phosphorylation. It should be noted that the modification of the N protein, either by loss of the phosphate moiety or substitution of a Ser or Thr amino acid by alanine, did not affect the stability of N protein as determined by immunofluorescence (data not shown). The absence of any IBV N protein did not result in rescue.

The effect of the modified N protein was only transient as replication of the IBV infectious RNA, generated from the IBV cDNA by the T7 RNA polymerase, would ultimately lead to the generation of subgenomic mRNA capable of expressing wild-type N protein. The fact that IBV N protein is essential for rescue supports the observation that modified N proteins were still capable of initiating rescue and that phosphorylation is not absolutely required for this role. Interestingly, loss of the Thr^{378} and Ser^{379} phosphorylation site N_{AATS} compared to N_{SSAA} protein resulted in a 20-fold decrease in rescue potentially indicating a more dominant role for this cluster site. Interestingly, this cluster site was also dominant in discriminating binding of the N protein to non-viral-derived RNA.

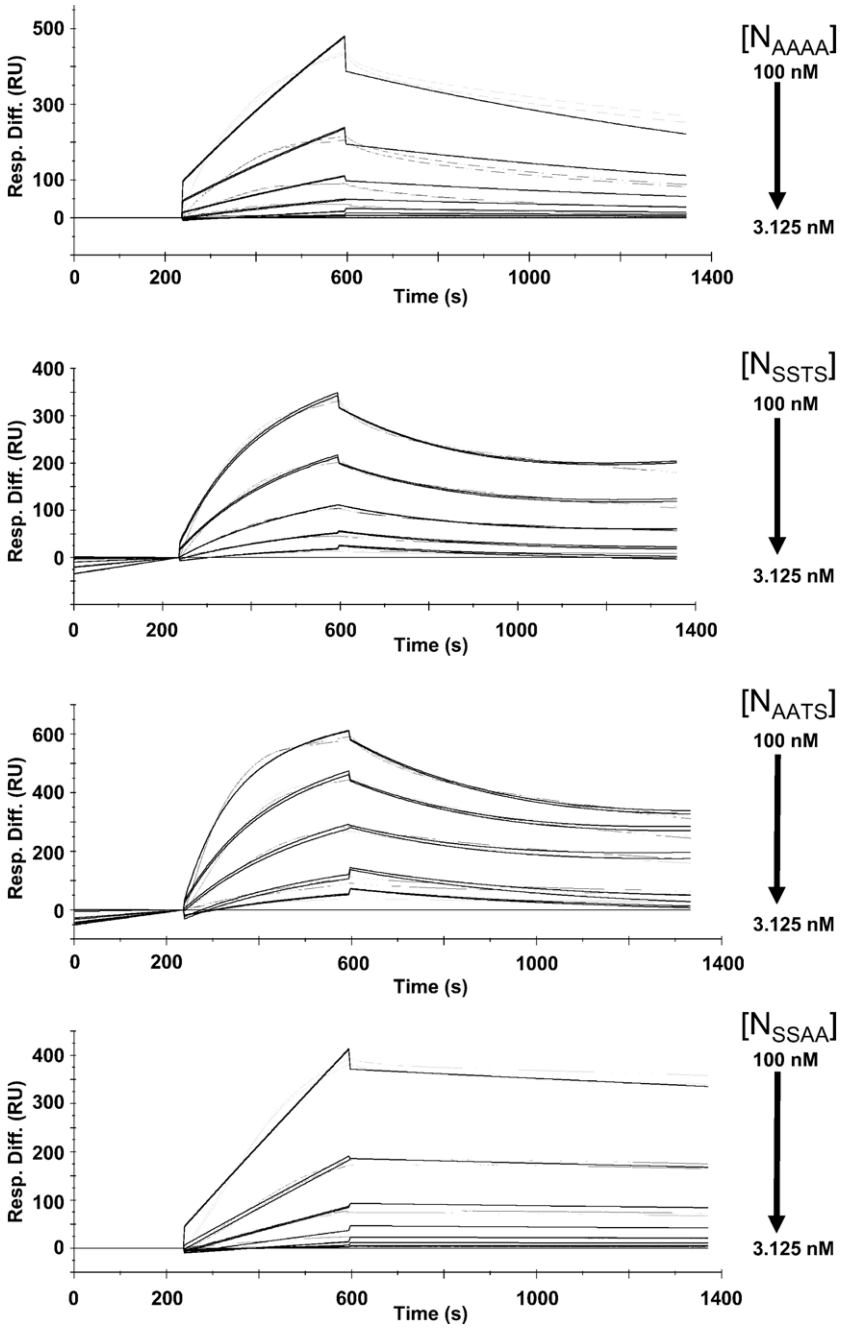

Fig. 3. Kinetic analyses of IBV N protein and the N proteins with modified phosphorylation sites binding to non-viral RNA. The proteins at 3.125, 6.25, 12.5, 25, 50 and 100 nM concentrations were injected over the immobilized RNA; association was monitored for 6 min followed by a 12 min dissociation phase. Black lines represent fitted data. Kinetic parameters for the experiments are shown in Table 1.

Our results indicated that the phosphorylation status of the IBV N protein may play a role in the virus life cycle and that the Thr^{378} and Ser^{379} residues appear to have the greatest influence on this role from the RNA binding studies and the ability of IBV N protein to initiate rescue of infectious virus from cDNA. These residues are located in the C-terminal region of the protein, the structure of which has been partially solved by X-ray crystallography using the Gray strain of IBV (Jayaram et al., 2006). Unfortunately, the portion of the protein for which the structure was solved encompasses residues 219 to 349 inclusive. The Thr^{378} and Ser^{379} residues lay outside of this fragment, and as such their position on the three dimensional model cannot be mapped. However, this region of the protein is reported to be stable and to contain a number of conserved residues (Jayaram et al., 2006), for example a nuclear export signal (Reed et al., 2007) which is shared with the SARS-CoV N protein (You et al., 2007). The Ser^{190} and Ser^{192} residues lie within the central region of the protein, the structure of which has not been elucidated. This region of the protein has been reported as intrinsically highly disordered (Enjuanes et al., 2006b; Jayaram et al., 2006) and as such difficult to purify and perform structural analysis. The observation that phosphoryla-

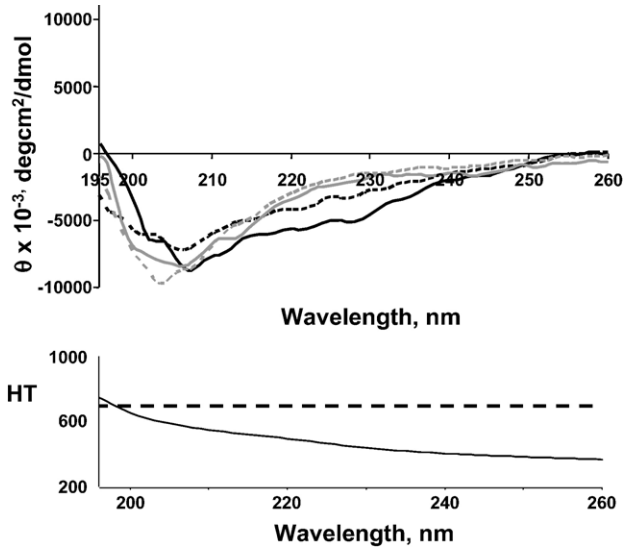

Fig. 4. CD spectroscopy of the IBV N proteins. The IBV N protein (N_{SSTS}) is shown by an unbroken black line, the modified N proteins, N_{AAAA} protein by a black dotted line, N_{AATS} protein by a gray dotted line and N_{SSAA} protein by a gray unbroken line. All the CD spectra were determined at the far UV (195–260 nm) wavelength. Shown beneath is the voltage at a given absorbance (continuous line).

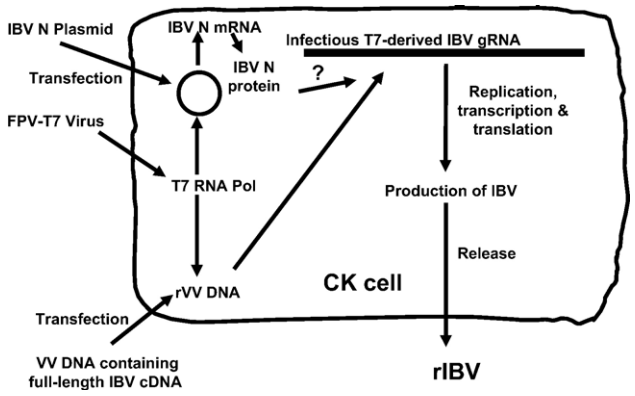

Fig. 5. Diagrammatic strategy for the recovery of infectious IBV from a full-length cDNA template. Expression of the IBV N protein from an expression plasmid is essential for the successful rescue of infectious IBV. Vaccinia virus DNA, containing the full-length IBV cDNA, and the plasmid expressing the IBV N genes are co-transfected into chick kidney cells previously infected with a recombinant fowlpox virus expressing T7 RNA polymerase. Expression of T7 RNA polymerase from the recombinant fowlpox virus results in the synthesis of infectious IBV RNA from the vaccinia virus DNA. The IBV RNA acts as an mRNA for the synthesis of the IBV replicase proteins, resulting in replication of the IBV RNA and generation of the subgenomic mRNAs for translation of the structural proteins and assembly of infectious virus progeny. The expression of IBV N protein from the co-transfected plasmid is required to initiate this process by an as yet unknown mechanism.

tion of residues in this disordered region has less of an effect on RNA binding ability than those in the structured C-terminal region indicates that the central region of the protein may indeed be unstructured and that changes, such as phosphorylation, have little effect on the function in this part of the protein.

Overall the phosphorylation status of IBV N protein has a dramatic influence on RNA binding capability and virus biology and that phosphorylation of only a small number of residues confers to N protein the ability to distinguish viral RNA from non-viral RNA. The mechanism by which this biological process occurs remains elusive, however, changes in RNA binding caused by a gross conformational change, upon phosphorylation of the protein, can be ruled out as playing a role in this complex viral process.

Materials and methods

Recombinant plasmids and baculoviruses

The IBV N protein was cloned C-terminal of a his-tag for expression in *E. coli* and insect cells as described previously (Chen et al., 2003, 2005). This plasmid served as template for the generation of plasmids that when expressed would lead to phosphorylation mutants of N protein. Specific mutations were introduced using the Stratagene QuikChange site directed mutagenesis kit. Three plasmids were generated $pTriExIBVN_{SSAA}$, $pTriExIBVN_{AATS}$ and $pTriExIBVN_{AAAA}$, which lead to the replacement of Thr^{378} and Ser379 with alanine, Ser190 and Ser^{192} with alanine and Ser190, Ser^{192}, Thr^{378} and Ser^{379} with alanine, respectively. Primer sequences are available on request. All constructs were sequenced in both directions. Recombinant baculoviruses were generated by transfecting Sf9 cells with the plasmids expression vector (which contained segments of baculovirus genomic DNA) and BacVector-3000 Triple Cut Virus DNA (Novagen). After transfection, monolayers were plaque assayed and candidate plaques individually purified by re-plaquing. Virus was harvested from subsequent plaques and used to infect exponentially growing cultures of Sf9 cells. These modified N protein genes were also cloned into the eukaryotic expression plasmid pCi-Neo that did not contain a his-tag moiety for rescue of infectious IBV as described (Casais et al., 2003, 2001). These vectors were pCi-$NeoIBVN_{SSAA}$, pCi-$NeoIBVN_{AATS}$ and pCi-$NeoIBVN_{AAAA}$. The cloning of wild-type N protein into pCi-Neo (in this study referred to as pCi-$NeoIBVN_{SSTS}$) has been described previously (Hiscox et al., 2001).

Table 2
Calculation of secondary structure elements of differentially phosphorylated IBV N protein

	α-Helix	β-Sheet	β-Turn	Random coil	NMRSD
N_{SSTS}	20±4	33±7	21±6	26±4	0.051
N_{AATS}	21±3	30±5	23±3	26±2	0.016
N_{SSAA}	20±2	31±4	22±5	17±1	0.034
N_{AAAA}	18±2	33±8	22±4	27±2	0.021

Analysis was performed using the CDSSTR method of three separate readings and averages calculated; errors are displayed as deviation from the mean.

Expression and purification of recombinant protein from Sf9 cells

Sf9 suspension cells were infected with the appropriate baculovirus expressing either the wild-type N protein or mutant N protein at an MOI of 5. Cultures were grown for 48 h and cell pellets were harvested by centrifugation. Cell pellets were

resuspended in RIPA lysis buffer and insoluble debris removed by high speed centrifugation. The soluble fraction containing the N protein was purified using column chromatography as described (Chen et al., 2003, 2005; Spencer and Hiscox, 2006b).

Surface plasmon resonance (SPR)

SPR measurements were conducted on a Biacore3000 instrument as previously described (Chen et al., 2005) and data fitted to a 1:1 Langmuir model. Briefly, a biotinylated RNA was immobilized on a streptavidin sensor chip (BIAcore) and varying concentrations of the N protein or mutants passed over, with a flow rate of 30 μl/min. Mass transport analysis experiments were conducted as described previously and no effects were observed.

RNA synthesis

Two RNA templates were used for SPR analysis in this study. In this system the IBV subgenomic mRNA 3 leader sequence was used as a viral target for N protein. The chemically synthesized RNA consisted of a biotin group at the 5′ end followed by the 90 nucleotide leader sequence up to and including a translation initiation codon (Chen et al., 2005; Spencer and Hiscox, 2006a,b). Biotin-ACUUAAGAUAGA-UAUUAAUAUAUAUCUAUUACACUAGCCUUGCGCUA-GAUUUUUAACUGAACAAUACAGACCUAAAAAGUCU-GUUUGAUG. The TRS is shown in bold face. The non-viral RNA was synthesized by *in vitro* transcription and biotin was incorporated at the 5′ end as part of this reaction. The sequence was GGGAGCUCCAGAAGAUAAAUUACAGG-UCGUAG-CAUAGUUAUUAGUCCAGAGAUGUUGAGA-GAUA-CAGCGCAGUCUCCAACUAGGAUACUAUG-ACCCC.

Circular dichroism

CD experiments were performed on a Jasco J715 spectrophotometer. Protein samples to be analyzed were dialyzed into 20 mM sodium phosphate buffer, pH 7.2. Measurements were taken in the far-UV (195–260 nm) and the CD signal recorded in a 1-mm path-length cell using a protein concentration of 0.4, 0.6 and 0.8 mg/ml with eight accumulations.

Acknowledgments

This research was supported by a BBSRC DTA/CASE studentship with Guildhay UK Ltd to KS. MD was supported by a joint IAH/Reading University studentship. The authors would like to acknowledge Andy Baron for help with SPR, Dr Paul Digard for the generous donation of pcDNA2.1-NP-wt and Drs John McCauley and Craig Ross for the generous donation of pEF6A-BVDV-capsid.

References

Almazan, F., Galan, C., Enjuanes, L., 2004. The nucleoprotein is required for efficient coronavirus genome replication. J. Virol. 78, 12683–12688.

Alonso, S., Izeta, A., Sola, I., Enjuanes, L., 2002. Transcription regulatory sequences and mRNA expression levels in the coronavirus transmissible gastroenteritis virus. J. Virol. 76, 1293–1308.

Baric, R.S., Nelson, G.W., Fleming, J.O., Deans, R.J., Keck, J.G., Casteel, N., Stohlman, S.A., 1988. Interactions between coronavirus nucleocapsid protein and viral RNAs—implications for viral transcription. J. Virol. 62, 4280–4287.

Britton, P., Evans, S., Dove, B., Davies, M., Casais, R., Cavanagh, D., 2005. Generation of a recombinant avian coronavirus infectious bronchitis virus using transient dominant selection. J. Virol. Methods 123, 203–211.

Calvo, E., Escors, D., Lopez, J.A., Gonzalez, J.M., Alvarez, A., Arza, E., Enjuanes, L., 2005. Phosphorylation and subcellular localization of transmissible gastroenteritis virus nucleocapsid protein in infected cells. J. Gen. Virol. 86, 2255–2267.

Casais, R., Theil, V., Siddell, S.G., Cavanagh, D., Britton, P., 2001. Reverse genetics system for the avian coronavirus infectious bronchitis virus. J. Virol. 75, 12359–12369.

Casais, R., Dove, B., Cavanagh, D., Britton, P., 2003. Recombinant avian infectious bronchitis virus expressing a heterologous spike gene demonstrates that the spike protein is a determinant of cell tropism. J. Virol. 77, 9084–9089.

Cavanagh, D., 2005. Coronaviruses in poultry and other birds. Avian Pathol. 34, 439–448.

Cawood, R., Harrison, S.M., Dove, B.K., Reed, M.L., Hiscox, J.A., 2007. Cell cycle dependent localisation of the coronavirus nucleocapsid protein. Cell Cycle 6, 863–867.

Chen, H., Wurm, T., Britton, P., Brooks, G., Hiscox, J.A., 2002. Interaction of the coronavirus nucleoprotein with nucleolar antigens and the host cell. J. Virol. 76, 5233–5250.

Chen, H., Coote, B., Attree, S., Hiscox, J.A., 2003. Evaluation of a nucleoprotein-based enzyme-linked immunosorbent assay for the detection of antibodies against infectious bronchitis virus. Avian Pathol. 32, 519–526.

Chen, H., Gill, A., Dove, B.K., Emmett, S.R., Kemp, F.C., Ritchie, M.A., Dee, M., Hiscox, J.A., 2005. Mass spectroscopic characterisation of the coronavirus infectious bronchitis virus nucleoprotein and elucidation of the role of phosphorylation in RNA binding using surface plasmon resonance. J. Virol. 79, 1164–1179.

Coley, S.E., Lavi, E., Sawicki, S.G., Fu, L., Schelle, B., Karl, N., Siddell, S.G., Thiel, V., 2005. Recombinant mouse hepatitis virus strain A59 from cloned, full-length cDNA replicates to high titers in vitro and is fully pathogenic in vivo. J. Virol. 79, 3097–3106.

Denison, M.R., Spaan, W.J.M., vanderMeer, Y., Gibson, C.A., Sims, A.C., Prentice, E., Lu, X.T., 1999. The putative helicase of the coronavirus mouse hepatitis virus is processed from the replicase gene polyprotein and localizes in complexes that are active in viral RNA synthesis. J. Virol. 73, 6862–6871.

Dove, B., Brooks, G., Bicknell, K., Wurm, T., Hiscox, J.A., 2006. Cell cycle perturbations induced by infection with the coronavirus infectious bronchitis virus and their effect on virus replication. J. Virol. 80, 4147–4156.

Enjuanes, L., Almazan, F., Sola, I., Zuniga, S., 2006a. Biochemical aspects of coronavirus replication and virus–host interaction. Annu. Rev. Microbiol. 60, 211–230.

Enjuanes, L., Almazan, F., Sola, I., Zuniga, S., Alvarez, E., Reguera, J., Capiscol, C., 2006b. Biochemical aspects of coronavirus replication. Adv. Exp. Med. Biol. 581, 13–24.

Fan, H., Ooi, A., Tan, Y.W., Wang, S., Fang, S., Liu, D.X., Lescar, J., 2005. The nucleocapsid protein of coronavirus infectious bronchitis virus: crystal structure of its N-terminal domain and multimerization properties. Structure 13, 1859–1868.

Fouts, D.E., True, H.L., Cengel, K.A., Celander, D.W., 1997. Site-specific phosphorylation of the human immunodeficiency virus type-1 Rev protein accelerates formation of an efficient RNA-binding conformation. Biochemistry 43, 13256–13262.

Greatorex, J.S., Palmer, E.A., Pomerantz, R.J., Dangerfield, J.A., Lever, A.M., 2006. Mutation of the Rev-binding loop in the human immunodeficiency virus 1 leader causes a replication defect characterized by altered RNA trafficking and packaging. J. Gen. Virol. 87, 3039–3044.

Hiscox, J.A., 2007. RNA viruses: hijacking the dynamic nucleolus. Nat. Rev., Microbiol. 5, 119–127.

Hiscox, J.A., Mawditt, K.L., Cavanagh, D., Britton, P., 1995. Investigation of the control of coronavirus subgenomic mRNA transcription by using T7-generated negative-sense RNA transcripts. J. Virol. 69, 6219–6227.

Hiscox, J.A., Wurm, T., Wilson, L., Cavanagh, D., Britton, P., Brooks, G., 2001. The coronavirus infectious bronchitis virus nucleoprotein localizes to the nucleolus. J. Virol. 75, 506–512.

Ivanov, K.I., Puustinen, P., Mertis, A., Saarma, M., Makinen, K., 2001. Phosphorylation down-regulates the RNA binding function of the coat protein of potato virus A. J. Biol. Chem. 276, 13530–13540.

Jayaram, J., Youn, S., Collisson, E.W., 2005. The virion N protein of infectious bronchitis virus is more phosphorylated than the N protein from infected cell lysates. Virology 339, 127–135.

Jayaram, H., Fan, H., Bowman, B.R., Ooi, A., Jayaram, J., Collisson, E.W., Lescar, J., Prasad, B.V., 2006. X-ray structures of the N- and C-terminal domains of a coronavirus nucleocapsid protein: implications for nucleocapsid formation. J. Virol. 80, 6612–6620.

Johnson, W.C., 1999. Analyzing protein circular dichroism spectra for accurate secondary structures. Proteins 35, 307–312.

Law, L.M., Everitt, J.C., Beatch, M.D., Holmes, C.F., Hobman, T.C., 2003. Phosphorylation of rubella virus capsid regulates its RNA binding activity and virus replication. J. Virol. 77, 1764–1771.

Masters, P.S., 2006. The molecular biology of coronaviruses. Adv. Virus. Res. 66, 193–292.

Mir, M.A., Panganiban, A.T., 2006. Characterization of the RNA chaperone activity of hantavirus nucleocapsid protein. J. Virol. 80, 6276–6285.

Mir, M.A., Brown, B., Hjelle, B.L., Duran, W.A., Panganiban, A.T., 2006. Hantavirus N protein exhibits genus-specific recognition of the vRNA panhandle. J. Virol. 80, 11283–11292.

Nelson, G.W., Stohlman, S.A., Tahara, S.M., 2000. High affinity interaction between nucleocapsid protein and leader/intergenic sequence of mouse hepatitis virus RNA. J. Gen. Virol. 81, 181–188.

Parker, M.M., Masters, P.S., 1990. Sequence comparison of the N genes of 5 strains of the coronavirus mouse hepatitis-virus suggests a 3 domain-structure for the nucleocapsid protein. Virology 179, 463–468.

Pasternak, A.O., Spaan, W.J., Snijder, E.J., 2006. Nidovirus transcription: how to make sense? J. Gen. Virol. 87, 1403–1421.

Peiris, J.S., Guan, Y., Yuen, K.Y., 2004. Severe acute respiratory syndrome. Nat. Med. 10, S88–S97.

Reed, M.L., Dove, B.K., Jackson, R.M., Collins, R., Brooks, G., Hiscox, J.A., 2006. Delineation and modelling of a nucleolar retention signal in the coronavirus nucleocapsid protein. Traffic 7, 833–848.

Reed, M.L., Howell, G., Harrison, S.M., Spencer, K.A., Hiscox, J.A., 2007. Characterization of the nuclear export signal in the coronavirus infectious bronchitis virus nucleocapsid protein. J. Virol. 81, 4298–4304.

Sawicki, S.G., Sawicki, D.L., Siddell, S.G., 2007. A contemporary view of coronavirus transcription. J. Virol. 81, 20–29.

Schelle, B., Karl, N., Ludewig, B., Siddell, S.G., Thiel, V., 2005. Selective replication of coronavirus genomes that express nucleocapsid protein. J. Virol. 79, 6620–6630.

Sola, I., Moreno, J.L., Zuniga, S., Alonso, S., Enjuanes, L., 2005. Role of nucleotides immediately flanking the transcription-regulating sequence core in coronavirus subgenomic mRNA synthesis. J. Virol. 79, 2506–2516.

Spencer, K.A., Hiscox, J.A., 2006a. Characterisation of the RNA binding properties of the coronavirus infectious bronchitis virus nucleocapsid protein amino-terminal region. FEBS Lett. 580, 5993–5998.

Spencer, K.A., Hiscox, J.A., 2006b. Expression and structural analysis of infectious bronchitis virus nucleoprotein. Adv. Exp. Med. Biol. 581, 133–138.

Stohlman, S.A., Baric, R.S., Nelson, G.N., Soe, L.H., Welter, L.M., Deans, R.J., 1988. Specific interaction between coronavirus leader RNA and nucleocapsid protein. J. Virol. 62, 4288–4295.

Surjit, M., Kumar, R., Mishra, R.N., Reddy, M.K., Chow, V.T., Lal, S.K., 2005. The severe acute respiratory syndrome coronavirus nucleocapsid protein is phosphorylated and localizes in the cytoplasm by 14-3-3-mediated translocation. J. Virol. 79, 11476–11486.

Tan, Y.W., Fang, S., Fan, H., Lescar, J., Liu, D.X., 2006. Amino acid residues critical for RNA-binding in the N-terminal domain of the nucleocapsid protein are essential determinants for the infectivity of coronavirus in cultured cells. Nucleic Acid Res. 34, 4816–4825.

van der Meer, Y., Snijder, E.J., Dobbe, J.C., Schleich, S., Denison, M.R., Spaan, W.J.M., Locker, J.K., 1999. Localization of mouse hepatitis virus nonstructural proteins and RNA synthesis indicates a role for late endosomes in viral replication. J. Virol. 73, 7641–7657.

van Marle, G., Luytjes, W., van der Most, R., van der Straaten, T., Spaan, W.J.M., 1995. Regulation of coronavirus mRNA transcription. J. Virol. 69, 7851–7856.

White, T.C., Yi, Z., Hogue, B.G., 2007. Identification of mouse hepatitis coronavirus A59 nucleocapsid protein phosphorylation sites. Virus Res. 126, 139–148.

Whitmore, L., Wallace, B.A., 2004. DICHROWEB, an online server for protein secondary structure analyses from circular dichroism spectroscopic data. Nucleic Acid Res. 32, W668–W673.

You, J., Dove, B.K., Enjuanes, L., DeDiego, M.L., Alvarez, E., Howell, G., Heinen, P., Zambon, M., Hiscox, J.A., 2005. Subcellular localization of the severe acute respiratory syndrome coronavirus nucleocapsid protein. J. Gen. Virol. 86, 3303–3310.

You, J.H., Reed, M.L., Hiscox, J.A., 2007. Trafficking motifs in the SARS-coronavirus nucleocapsid protein. Biochem. Biophys. Res. Commun. 358, 1015–1020.

Youn, S., Collisson, E.W., Machamer, C.E., 2005a. Contribution of trafficking signals in the cytoplasmic tail of the infectious bronchitis virus spike protein to virus infection. J. Virol. 79, 13209–13217.

Youn, S., Leibowitz, J.L., Collisson, E.W., 2005b. In vitro assembled, recombinant infectious bronchitis viruses demonstrate that the 5a open reading frame is not essential for replication. Virology 332, 206–215.

Yount, B., Curtis, K.M., Baric, R.S., 2000. Strategy for systematic assembly of large RNA and DNA genomes: transmissible gastroenteritis virus model. J. Virol. 74, 10600–10611.

Yount, B., Curtis, K.M., Fritz, E.A., Hensley, L.E., Jahrling, P.B., Prentice, E., Denison, M.R., Geisbert, T.W., Baric, R.S., 2003. Reverse genetics with a full-length infectious cDNA of severe acute respiratory syndrome coronavirus. Proc. Natl. Acad. Sci. USA 100, 12995–13000.

Yu, M., Summers, J., 1994. Phosphorylation of the duck hepatitis B virus capsid protein associated with conformational changes in the C terminus. J. Virol. 68, 2965–2969.

Zuniga, S., Sola, I., Alonso, S., Enjuanes, L., 2004. Sequence motifs involved in the regulation of discontinuous coronavirus subgenomic RNA synthesis. J. Virol. 78, 980–994.

Zuniga, S., Sola, I., Moreno, J.L., Sabella, P., Plana-Duran, J., Enjuanes, L., 2007. Coronavirus nucleocapsid protein is an RNA chaperone. Virology 20, 215–227.